Macromolecular Rapid Communication
www.mrc-journal.de

Influence of Chemical and Physical Change of Pollen Microgels on Swelling/De-Swelling Behavior

*Teng-Fei Fan, Youngkyu Hwang, Mohammed Shahrudin Ibrahim, Gaia Ferracci, and Nam-Joon Cho**

Pollen, the male microgametophyte of seed plants, is commonly used as a food and health supplement. Here, a facile method to transform sunflower pollen into pH-responsive microgels with tailored properties is presented. The structure and morphology of the pollen microgel are characterized by scanning electron microscopy, confocal laser scanning microscopy, and dynamic image particle analysis based on potassium hydroxide treatment with various incubation time and concentration. These pollen microgels exhibit significant volume change under different pH conditions and Ca^{+}/ethylenediaminetetraacetic acid treatment. The results describe the fundamental properties of pollen microgels and pave the way for its future applications, such as "smart" drug carriers.

1. Introduction

Pollen is the male reproductive organ of seed plants, which is also known as the toughest material in the plant world due to its indestructible pollen wall.[1,2] Pollen wall plays important roles to protect the reproductive cells from the desiccation and microorganism.[3,4] Geometrically, the pollen wall is composed of two layers: a tough sporopollenin-based exine layer and a soft polysaccharide-based intine layer.[1,5–7] The exine layer is naturally a unique microcapsule that possesses many special properties such as ultraviolet light shielding, antioxidant, elastic, and physical–chemical resilience.[8–10] The microstructure of the pollen surface is one of the key characters for pollen species identification. The number, position, and shape of the pollen aperture are also species-specific and play dominant roles in the pollen hydration and dehydration procedures.[6,11]

Flower pollen particles are eco-friendly, biocompatible, and abundant and have attracted considerable interest as a drug carrier,[12–18] biotemplate,[19,20] polymer filler,[21,22] biosensors,[23,24] and micromotors.[25,26] The hollow structure and uniform size of pollen particles provide many advantages for the medical applications as a carrier, such as a large volume of the cavity and low cost for preparation.[27–30] However, mechanical and chemical stability of the pollen particles restricts further development due to low processability. Recently, we developed the soapmaking-like process to transform the pollen particles into the pollen microgels, which show great potential as a functional carrier for drug/protein delivery.[31] The pollen microgel particles also show pH- and ion- responsive swelling/deswelling behavior. The de-esterification of pectin in the intine layer plays an important role in pollen gelation behavior.[32,33] We previously reported that 6 species of pollen were successfully transformed into pH-responsive microgels without destroying the morphology of the pollen wall.[31] However, the influence of parameters involved in the synthesis on the physical and chemical properties of the pollen microgel are still unknown.

In this study, we address the physical and chemical properties of the sunflower pollen microgel, depending on various conditions. Dynamic image particle and fourier-transform infrared spectroscopy (FTIR) analysis show the geometrical and chemical change of pollen microgel as various incubation time and concentration of potassium hydroxide (KOH) solution. Increasing the carboxyl moiety in pectin enhances the swelling ratio, which resulted in a substantial volume change of pollen microgel for high drug loading capacity. In addition, cycling tests under different pH and Ca^{+}/ethylenediaminetetraacetic acid (EDTA) show the durability and feasibility of pollen microgel in a controllable manner.

2. Results and Discussion

The preparation of the pollen microgel begins with the removal of the cytoplasm of defatted sunflower grains (**Figure 1**). The

Dr. T.-F. Fan, Dr. Y. Hwang, M. S. Ibrahim, G. Ferracci, Prof. N.-J. Cho
School of Materials Science and Engineering
Nanyang Technological University
50, Nanyang Avenue 639798, Singapore
E-mail: njcho@ntu.edu.sg
Dr. Y. Hwang
School of Chemical Engineering
Sungkyunkwan University
Suwon 16229, Republic of Korea
Dr. Y. Hwang
Biomedical Institute for Convergence at SKKU (BICS)
Sungkyunkwan University
Suwon 16229, Republic of Korea
M. S. Ibrahim, G. Ferracci
Interdisciplinary Graduate School
NTU Institute for Health Technologies
Nanyang Technological University
50, Nanyang Avenue 639798, Singapore
The ORCID identification number(s) for the author(s) of this article can be found under https://doi.org/10.1002/marc.202000155.

DOI: 10.1002/marc.202000155

defatting process exposes the porous exine layer and aperture of the pollen grain (Figure 1a,d). In this step, protein, and lipid, which can cause allergic reaction, are removed. To remove the cytoplasm, we performed 10% w/v of KOH solution treatment at 80 °C for 2 h. A hot KOH solution induced cytoplasmic extrusion in a short period (within 2 h), and then the inner space of pollen grain was filled with KOH solution (Figure 1b,e). To confirm the removal of the pollen cytoplasm, we obtained the confocal laser scanning microscopy images of the defatted and KOH treated pollen grains (Figures S1 and S2, Supporting Information). Fluorescence signals from the whole pollen grains, including pollen wall and inner content (cytoplasm), were observed in the defatted samples. However, we only observed the fluorescence signals from the pollen wall in the pollen microgel samples, which is evidence that the cytoplasm materials were successfully removed after KOH treatment. Scanning electron microscopy (SEM) images also showed clear pores on the surface of the pollen grain due to the cavity in the pollen (Figure 1e). Further incubation of the pollen particles in 10% w/v of KOH solution at 80 °C induces the gelation of pollen grains by de-esterifying the pectin in the intine layer (Figure 1c). De-esterification resulted in an increase of the carboxyl group on the intine layer, which enables the gelation of the pollen grains.[34] We can observe the spike structure on the surface of the pollen microgel (Figure 1f). Thus, we conclude that the KOH treatment removes the inner content of the pollen grain but preserves the unique surface structure of the pollen shell.

To address the physical property of the pollen microgel, we treated the pollen microgel with various concentrations and the incubation time of the KOH solution. Regarding the concentration aspect, we incubated pollen microgel in the 10%, 20%, and 30% w/v of KOH solution for 24 h and then measured size change as a function of the different pH using the dynamic image particle analysis (DIPA) method. In the meantime, we can observe the morphology of pollen microgels at different conditions (Figure S3, Supporting Information). Pollen microgel with 10% w/v KOH treatment showed the largest change of diameter from 22.17 ± 1.52 to 52.48 ± 5.52 µm. As the concentration of KOH increases by up to 30%, the maximum diameter at pH 10 is 42.51 ± 2.68 (20%) and 40.56 ± 2.21 µm (30%) (**Figure 2a**). We believe this trend is due to the degradation of the pectin in the intine layer resulting in a decrease of the maximum diameter. As shown in earlier studies, pectin can be degraded through saponification and β-elimination in alkaline and high temperature (e.g., 80 °C) conditions.[35,36] Interestingly, all samples show the maximum diameter at pH 10 and then decrease it at pH 14. We believe the carboxyl groups of pectin is fully deprotonated at pH 10, but at pH 14, the excess of the K^+ ion in pH buffer solution (KOH in this study) can neutralize the negative charge of the carboxyl groups.[34] We also investigated the effect of the incubation time in 10% w/v KOH solution for the swelling/de-swelling behavior of pollen microgel (Figure 2b). The minimum diameters of pollen microgel after 6, 24, 48, and 90 h incubation are 22.84 ± 1.63, 22.17 ± 1.52, 22.38 ± 3.30, and 13.28 ± 2.15 µm in pH 2. In the case of 90 h incubation, pollen microgel shows a smaller diameter compared to other pollen microgels due to the degradation/destruction of pollen microgel. Those broken pollen pieces of 90 h samples still possess the pH-responsiveness, resulting in the smallest diameter of pollen microgel in pH 2. Pollen microgel after 24 h incubation in 10% w/v KOH has the largest diameter at pH 10 compared to those of pollen microgel

Fan Tengfei graduated from China Agricultural University and has been a postdoctoral researcher in the School of Resources and the Environment at China Agricultural University and now at the School of Materials and Engineering at Nanyang University of Technology. His research fields mainly include the development and application of pollen materials (especially pollen microgels), the preparation of polymer microcapsules and their application in agriculture, the effective transport of plant roots, the utilization of NH_4^+, NO_3^- genes, and their biological functions.

Youngkyu Hwang received his B.S. in life science from Kyunghee University, South Korea, in 2007. He then earned his doctorate in materials science and engineering from Gwangju Institute of Science and Technology, South Korea, in 2018. He continued his postdoctoral training in materials science and engineering at Nanyang Technological University in 2019. He joined Sungkyunkwan University as a postdoctoral fellow in 2020, and his latest research is focused on the fundamental study and applications of pollen grains.

Nam-Joon Cho is a professor in the School of Materials Science and Engineering at Nanyang Technological University. His group's research focuses on engineering approaches to solve important biomedical problems and to translate these capabilities into practical applications for global health. He also leads a multi-institution tissue engineering collaboration involving NTU and the Stanford University School of Medicine, which focuses on developing an artificial liver platform for regenerative medicine applications. He is a graduate of Stanford University and the University of California, Berkeley.

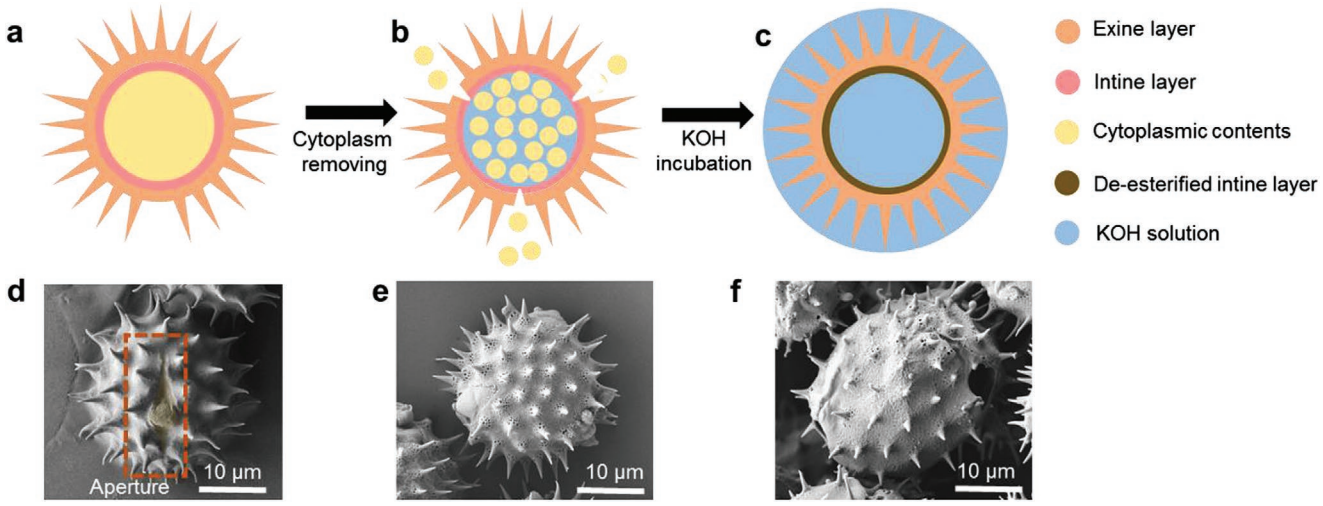

Figure 1. The strategy of transforming natural sunflower pollen grains into the pollen microgel. a) Intact single defatted sunflower pollen grain. b) The cytoplasm was removed from the pollen grain. c) Pollen microgel formed after KOH incubation. d) SEM image of defatted sunflower pollen grain with an open aperture. e) SEM image of a pollen grain after cytoplasm removal. f) SEM image of freeze-dried pollen microgel.

after 6, 48, and 90 h incubation. 48 and 90 h-treated pollen microgel shows the slight decreases of the maximum diameter because the degradation of pectin leads to the decrease of the internal force to swell the pollen microgel.[37] 6 h-treated pollen microgel also shows a smaller maximum diameter at pH 10. This is because the stiff pollen shell restricts the swelling of the pollen microgel.[31] These results indicate that two processes control the volume change of the pollen microgel. 1) The deprotonation of the carboxyl group in pectin acts a key role to provide the internal force for swelling/de-swelling. 2) The

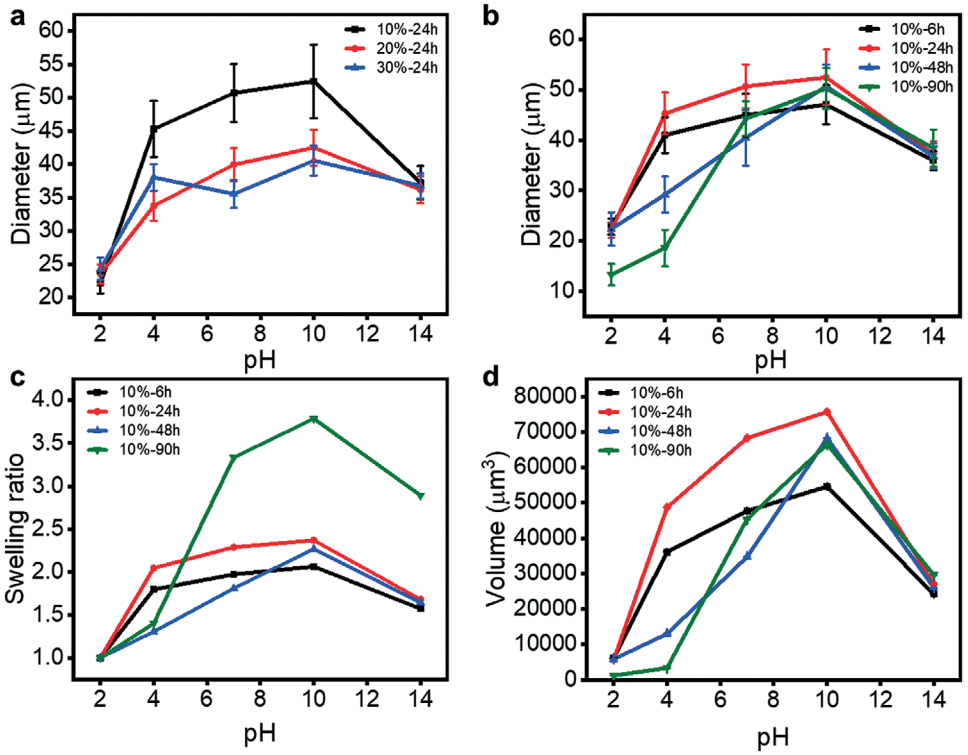

Figure 2. pH-dependent swelling–de-swelling behavior of sunflower pollen microgel. a) Influence of pH on the size of sunflower pollen microgel prepared with different concentrations of KOH solution (10%, 20%, and 30%). b) Influence of pH on the diameter of sunflower pollen microgel prepared with different incubation time (6, 24, 48, and 90 h) in 10% KOH solution. c) The swelling ratio of sunflower pollen microgel prepared with different incubation time (6, 24, 48, and 90 h) in 10% KOH solution. d) Influence of pH on the volume of sunflower pollen microgel prepared with different incubation time (6, 24, 48, and 90 h) in 10% KOH solution.

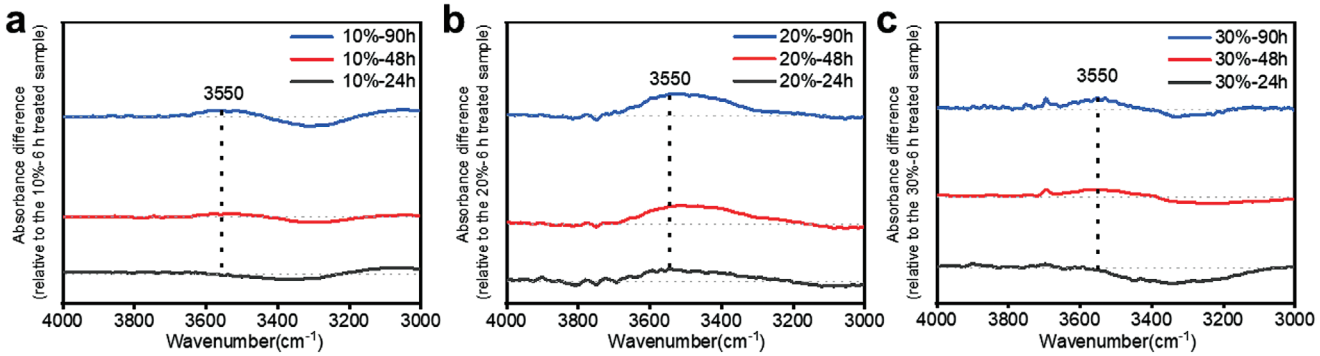

Figure 3. FTIR absorbance difference spectra of the sunflower pollen microgel after different KOH treatment showing the mean spectrum minus the mean spectrum of samples treated for 6 h. a) Absorbance difference spectra of the sunflower pollen microgel treated with 10% aqueous KOH for 24, 48, and 90 h. b) Absorbance difference spectra of the sunflower pollen microgel treated with 20% KOH aqueous for 24, 48, and 90 h. c) Absorbance difference spectra of the sunflower pollen microgel treated with 30% KOH aqueous for 24, 48, and 90 h. Grey dashed line indicates no shift (i.e., no difference between experimental samples and 6 h treated sample).

stiffness of the exine layer determines the maximum diameter of the pollen microgel. We further calculated the swelling ratio (the minimum diameter divided by the maximum diameter) of the pollen microgel. The swelling ratio of the pollen microgel is 2.0 (6 h), 2.4 (24 h), 2.3 (48 h), and 3.8 (90 h) (Figure 2c). The highest swelling ratio in 90 h-treated pollen microgel is contributed to the fractured pollen shells, which resulted in the small minimum diameter of pollen microgel in pH 2. We also calculated the maximum volume of the pollen microgel (Figure 2d). The maximum volume of the pollen microgel (minimum volume) is 54 605 μm^3 (6239 μm^3) of 6 h-treated sample, 75 680 μm^3 (5706 μm^3) of 24 h-treated sample, 68 237 μm^3 (5869 μm^3) of 48 h-treated sample, and 66 556 μm^3 (1226 μm^3) of 90 h-treated sample. In the case of the 24 h-treated pollen microgel in a 10% KOH solution, the volume of the swelling state is 13 times higher than the de-swelling state.

In order to quantify the changes of carboxyl groups of pollen microgel, we performed the FTIR using the freeze-dried samples after KOH treatment. **Figure 3** shows the absorbance spectra of 24, 48, and 90 h-treated samples in 10%, 20%, and 30% w/v KOH solution, which is normalized by that of 6 h-treated samples from 4000 to 3000 cm^{-1}, respectively. Although the peaks between 3500 and 3600 cm^{-1} corresponding to O—H bonds in carboxyl groups shows negligible changes in 10%-24 h and 10%-48 h-treated pollen microgel, pollen microgel in other conditions showed a positive shift in 3550 cm^{-1}.[38,39] This result implies that the longer incubation time and high KOH concentration induce more O—H groups in pectin. Additionally, longer incubation time (from 6 to 90 h) and the higher concentration of KOH (from 10% to 30% w/v) generate the color change from pale yellow to dark brown. The increase of peak at 1581 and 1584 cm^{-1} suggests that the formation of C=C bonds causes the color change in aromatic rings of sporopollenin (Figure S4, Supporting Information).[40] The peaks after 6 h incubation shifted to the higher wavenumber after 90 h incubation; 1071 cm^{-1} (1053 cm^{-1}) in 10% w/v KOH, 1071 cm^{-1} (1049 cm^{-1}) in 20% KOH, and 1068 cm^{-1} (1041 cm^{-1}) in 30% w/v KOH. That result infers the degradation of pectin in the pollen wall, especially from the intine layer.[41]

To demonstrate the durability, we performed the cycling test using 24 h-treated pollen microgel in a 10% KOH solution. Time-lapsed optical microscopy images show the dynamic swelling/de-swelling behavior of individual pollen microgel according to the pH change (pH 10 to pH 2 and pH 2 to pH 10) (**Figure** 4a). Fully swelled pollen microgel in pH 10 solution is rapidly de-swelled in 3 s after applying the HCl solution (pH 2). De-swelled pollen microgel is fully recovered to the swelling state by applying the KOH solution (pH 10). In addition, maximum and minimum are on the other way round (Figure 4b).

To demonstrate a controllable way for swelling/de-swelling behavior, we tested the chemical response of pollen microgel. As above mentioned, a negative charge of the carboxyl group in the intine generates the repulsion force, which leads to swelling of the pollen microgel. Therefore, the positive charges can reduce the repulsion force between the pectin polymers by the cancellation of the negative charge. We measured the diameter of pollen microgel, which are incubated for 6, 24, 48, and 90 h in 10% w/v KOH solution (**Figure 5a**). The minimum diameters

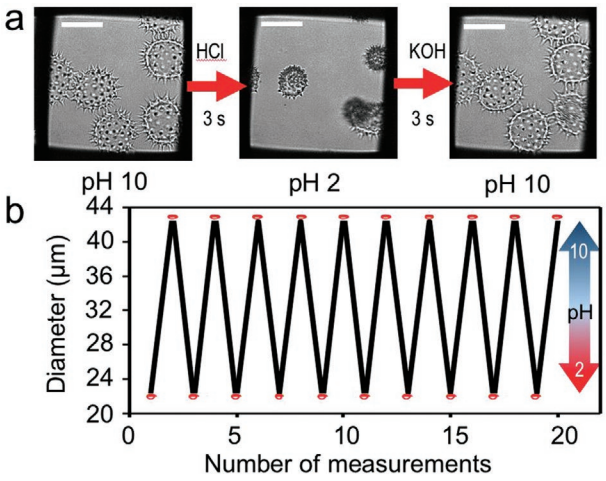

Figure 4. pH-dependent swelling–de-swelling behavior of sunflower pollen microgel. a) Time-lapsed optical micrographs of sunflower pollen microgel under pH 2 and pH 10. Scale bar: 50 μm. b) Swelling–de-swelling cycles of a single sunflower pollen microgel along with the pH changing between 2 to 10.

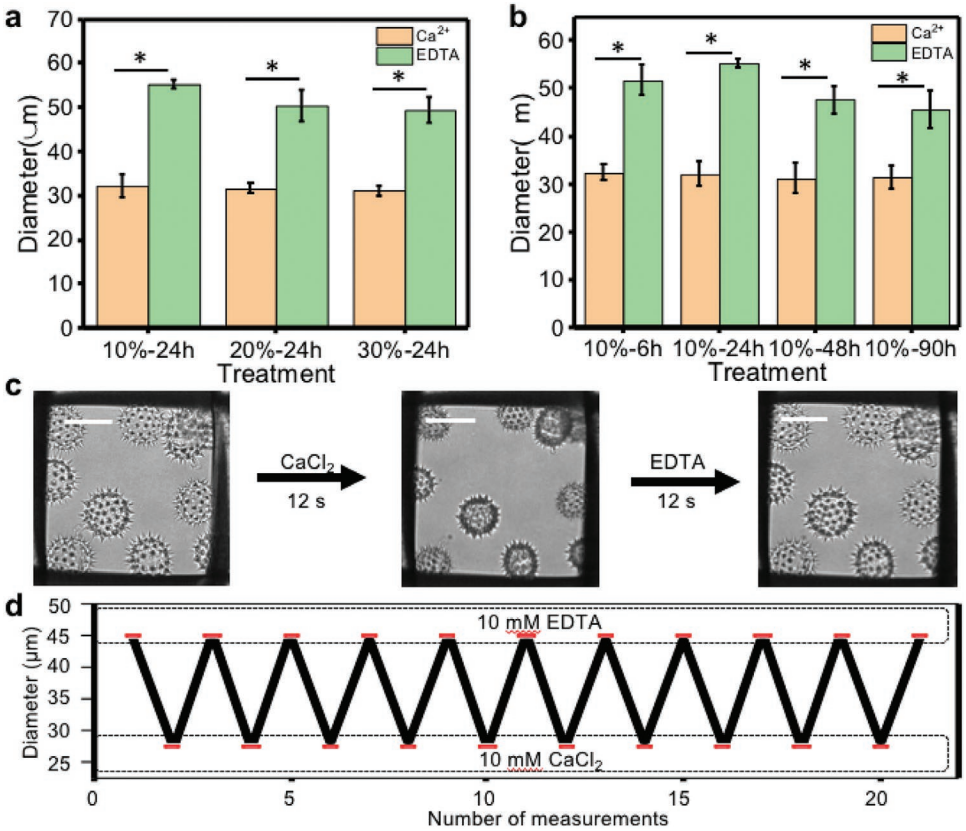

Figure 5. Ca^{2+}-EDTA induced swelling–de-swelling behavior of sunflower pollen microgel. a) Ca^{2+}-EDTA mediated the diameter of sunflower pollen microgel prepared with different concentrations of KOH solution (10%, 20%, and 30%). b) Ca^{2+}-EDTA mediated the diameter of sunflower pollen microgel prepared with different incubation time (6, 24, 48, 90 h). c) Time-lapsed optical micrographs of sunflower pollen microgel stimulated by Ca^{2+} (10 mM) and EDTA (10 mM). Scale bar: 50 μm. d) Swelling–de-swelling cycles of a single sunflower pollen microgel stimulated by Ca^{2+} (10 mM) and EDTA (10 mM).

of the pollen microgel are 32.44 ± 1.75 (6 h), 32.10 ± 2.61 (24 h), 32.25 ± 3.16 (48 h), and 31.47 ± 2.49 μm (90 h). The maximum diameters of the pollen microgel are 51.80 ± 3.25 (6 h), 55.20 ± 0.96 (24 h), 47.61 ± 2.94 (48 h), and 45.58 ± 3.86 μm (90 h). The DIPA data shows the calcium and EDTA response of pollen microgel (Figure 5b). The 10 mM of $CaCl_2$ solution induced the de-swelling of pollen microgel. The minimum diameters of 10, 20, and 30% w/v KOH solution treated pollen microgel are 32.1 ± 2.61, 31.58 ± 1.15, and 31.06 ± 1.09 μm. In addition, the pollen microgels are fully recovered by 10 mM of EDTA solution; The maximum diameters of the pollen microgel are 55.2 ± 0.96 (10%), 50.44 ± 3.54 (20%), and 49.46 ± 2.88 μm (30%). The pollen microgel shows good reversibility after multiple cycles of Ca^{2+} and EDTA treatment (Figure 5c); the diameter change of the pollen microgel is repeated from 27.50 to 45.00 μm. However, the Ca^{2+} response of the pollen microgel is slightly slower (12 s to "swell" and 12 s to "de-swell") than their pH response.

3. Conclusion

We address the physical and chemical property of the sunflower pollen microgel, which responds to pH and calcium ion. The swelling ratio of the pollen microgel can be easily modulated by adjusting KOH concentration and incubation time. 24 h-treated pollen microgel shows the maximum volume of 75 680 μm^3 in a single pollen microgel, which is higher than 27 000 μm^3 in non-gelated pollen microcapsules. The pollen microgels have biocompatibility, large swelling volume, and high uniformity, which is difficult to achieve using conventional methods. This will open new venues for microgel applications such as drug delivery, biosensor, and healthcare products.

Supporting Information

Supporting Information is available from the Wiley Online Library or from the author.

Acknowledgements

T.-F.F. and Y.H. contributed equally to this work. The NTU supported this work. This research was supported by the MOTIE (Ministry of Trade, Industry, and Energy) in Korea, under the Fostering Global Talents for Innovative Growth Program (P0008746) supervised by the Korea Institute for Advancement of Technology (KIAT).

Conflict of Interest

The authors declare no conflict of interest.

Keywords

pH responsiveness, pollen microgels, pollen walls, sunflower pollen

Received: March 26, 2020
Revised: May 9, 2020
Published online:

[1] G. Mackenzie, A. N. Boa, A. Diego-Taboada, S. L. Atkin, T. Sathyapalan, *Front. Mater.* **2015**, *2*, 66.
[2] J. M. Tylianakis, *Science* **2013**, *339*, 1532.
[3] H. J. B. Birks, H. H. Birks, B. Ammann, *Science* **2016**, *354*, 412.
[4] T. D. Quilichini, E. Grienenberger, C. J. Douglas, *Phytochemistry* **2015**, *113*, 170.
[5] T. I. Baskin, *Annu. Rev. Cell Dev. Biol.* **2005**, *21*, 203.
[6] E. Katifori, S. Alben, E. Cerda, D. R. Nelson, J. Dumais, *Proc. Natl. Acad. Sci. USA* **2010**, *107*, 7635.
[7] E. R. Rojas, S. Hotton, J. Dumais, *Biophys. J.* **2011**, *101*, 1844.
[8] G. Mackenzie, S. Beckett, S. Atkin, A. Diego-Taboada, in *Microencapsulation in the Food Industry*, Elsevier, Amsterdam **2014**, pp. 283–297.
[9] J. Brooks, G. Shaw, *Nature* **1968**, *219*, 532.
[10] T. Ariizumi, K. Toriyama, *Annu. Rev. Plant Biol.* **2011**, *62*, 437.
[11] E. Duhoux, *Grana* **1982**, *21*, 1.
[12] S. Barrier, *Ph.D. Thesis*, University of Hull **2008**.
[13] S. Barrier, A. S. Rigby, A. Diego-Taboada, M. J. Thomasson, G. Mackenzie, S. L. Atkin, *LWT–Food Sci. Technol.* **2010**, *43*, 73.
[14] L. J. Blackwell, *Ph.D. Thesis*, University of Hull **2007**.
[15] R. C. Mundargi, M. G. Potroz, J. H. Park, J. Seo, E.-L. Tan, J. H. Lee, N.-J. Cho, *Sci. Rep.* **2016**, *6*, 19960.
[16] R. C. Mundargi, M. G. Potroz, S. Park, H. Shirahama, J. H. Lee, J. Seo, N. J. Cho, *Small* **2016**, *12*, 1167.
[17] R. C. Mundargi, M. G. Potroz, S. Park, J. H. Park, H. Shirahama, J. H. Lee, J. Seo, N.-J. Cho, *Adv. Funct. Mater.* **2016**, *26*, 632.
[18] R. C. Mundargi, E.-L. Tan, J. Seo, N.-J. Cho, *J. Ind. Eng. Chem.* **2016**, *36*, 102.
[19] S. R. Hall, V. M. Swinerd, F. N. Newby, A. M. Collins, S. Mann, *Chem. Mater.* **2006**, *18*, 598.
[20] X. Yang, X. Song, Y. Wei, W. Wei, L. Hou, X. Fan, *Scr. Mater.* **2011**, *64*, 1075.
[21] J. H. Lee, B. M. Suttle, H. J. Kim, J. C. Meredith, *Macromol. Mater. Eng.* **2011**, *296*, 1055.
[22] O. O. Fadiran, J. C. Meredith, *J. Mater. Chem. A* **2014**, *2*, 17031.
[23] L. Wang, J. A. Jackman, W. B. Ng, N. J. Cho, *Adv. Funct. Mater.* **2016**, *26*, 8623.
[24] K. Tian, X.-X. Wang, H.-Y. Li, R. Nadimicherla, X. Guo, *Sens. Actuators, B* **2016**, *227*, 554.
[25] H. Wang, M. G. Potroz, J. A. Jackman, B. Khezri, T. Marić, N. J. Cho, M. Pumera, *Adv. Funct. Mater.* **2017**, *27*, 1702338.
[26] M. Sun, X. Fan, X. Meng, J. Song, W. Chen, L. Sun, H. Xie, *Nanoscale* **2019**, *11*, 18382.
[27] M. G. Potroz, R. C. Mundargi, J. J. Gillissen, E. L. Tan, S. Meker, J. H. Park, H. Jung, S. Park, D. Cho, S. I. Bang, *Adv. Funct. Mater.* **2017**, *27*, 1700270.
[28] A. K. Prabhakar, M. G. Potroz, E.-L. Tan, H. Jung, J. H. Park, N.-J. Cho, *ACS Appl. Mater. Interfaces* **2018**, *10*, 28428.
[29] E. L. Tan, M. G. Potroz, G. Ferracci, J. A. Jackman, H. Jung, L. Wang, N. J. Cho, *Adv. Funct. Mater.* **2018**, *28*, 1707568.
[30] R. C. Mundargi, M. G. Potroz, J. H. Park, J. Seo, J. H. Lee, N.-J. Cho, *RSC Adv.* **2016**, *6*, 16533.
[31] T.-F. Fan, S. Park, Q. Shi, X. Zhang, Q. Liu, Y. Song, H. Chin, M. S. B. Ibrahim, N. Mokrzecka, Y. Yang, *Nat. Commun.* **2020**, *11*, 1.
[32] M. Bosch, A. Y. Cheung, P. K. Hepler, *Plant Physiol.* **2005**, *138*, 1334.
[33] A. M. Vieira, J. A. Feijó, *Am. J. Bot.* **2016**, *103*, 437.
[34] J. B. Wehr, N. Menzies, F. Blamey, *Food Hydrocolloids* **2004**, *18*, 375.
[35] C. M. Renard, J.-F. Thibault, *Carbohydr. Res.* **1996**, *286*, 139.
[36] W. Sułkowski, D. Pentak, K. Nowak, A. Sułkowska, *J. Mol. Struct.* **2005**, *744*, 737.
[37] V. B. V. Maciel, C. M. Yoshida, T. T. Franco, *Carbohydr. Polym.* **2015**, *132*, 537.
[38] R. Gnanasambandam, A. Proctor, *Food Chem.* **2000**, *68*, 327.
[39] A. Balaria, S. Schiewer, *Sep. Purif. Technol.* **2008**, *63*, 577.
[40] B. Yule, S. Roberts, J. Marshall, *Org. Geochem.* **2000**, *31*, 859.
[41] J. V. Diaz, G. E. Anthon, D. M. Barrett, *J. Agric. Food Chem.* **2007**, *55*, 5131.